

Classical analogs of generalized purities, entropies, and logarithmic negativityBogar Díaz^{1,2,3,*}, Diego Gonzalez^{4,†}, Marcos J. Hernández^{5,‡} and J. David Vergara^{5,§}¹*Departamento de Matemáticas, Universidad Carlos III de Madrid, Avenida de la Universidad 30, 28911 Leganés, Spain*²*Grupo de Teorías de Campos y Física Estadística. Instituto Gregorio Millán (UC3M),**Unidad Asociada al Instituto de Estructura de la Materia, CSIC, Serrano 123, 28006 Madrid, Spain*³*Instituto de Ciencias Matemáticas (ICMAT), CSIC-UAM-UC3M-UCM, C. Nicolás Cabrera 13-15, 28049 Madrid, Spain*⁴*Escuela Superior de Ingeniería Mecánica y Eléctrica - Instituto Politécnico Nacional (ESIME - IPN), 07738, CDMX, Mexico*⁵*Departamento de Física de Altas Energías, Instituto de Ciencias Nucleares,**Universidad Nacional Autónoma de México, Apartado Postal 70-543, Ciudad de México, 04510, Mexico*

(Received 24 February 2023; accepted 6 June 2023; published 10 July 2023)

It has recently been proposed classical analogs of the purity, linear quantum entropy, and von Neumann entropy for classical integrable systems, when the corresponding quantum system is in a Gaussian state. We generalized these results by providing classical analogs of the generalized purities, Bastiaans-Tsallis entropies, Rényi entropies, and logarithmic negativity for classical integrable systems. These classical analogs are entirely characterized by the classical covariance matrix. We compute these classical analogs exactly in the cases of linearly coupled harmonic oscillators, a generalized harmonic oscillator chain, and a one-dimensional circular lattice of oscillators. In all of these systems, the classical analogs reproduce the results of their quantum counterparts whenever the system is in a Gaussian state. In this context, our results show that quantum information of Gaussian states can be reproduced by classical information.

DOI: [10.1103/PhysRevA.108.012411](https://doi.org/10.1103/PhysRevA.108.012411)**I. INTRODUCTION**

In recent times, many measures of quantum effects have emerged; among them, we can highlight the covariance matrix [1], purity [2], von Neumann entropy [3], Rényi entropies [4], Bastiaans-Tsallis entropies [5,6], logarithmic negativity [7,8], Berry phase [9], and quantum geometric tensor [10]. Each of these quantities has its utility since they easily discern specific characteristics of quantum phenomena. For instance, the von Neumann entropy encodes the degree of mixing of a quantum state. Also, the Rényi entropies are the natural generalization of the von Neumann entropy by deforming it into a parametrized entropy by a positive real number α , which characterizes different aspects of the entanglement spectrum in a similar way to higher moments of a probability distribution. Furthermore, the Rényi entropies have also found various applications [11]. In particular, these entropies are widely used as a technical tool in information theory [1], statistical mechanics [12], and recently using the maximum entropy principle applied to the Rényi entropies, a generalized formulation of quantum thermodynamics was developed [13].

In addition, the Rényi entropies have been essential to defining multifractality phenomena [14]. On the other hand, the Bastiaans-Tsallis entropies were introduced by Bastiaans in the context of quantum optics [5] and, independently, by Tsallis in statistical mechanics [6]. These entropies quantify the degree of mixedness of a state by the amount of information it lacks, and it is a nonadditive quantity. Also, it is a fundamental tool to describe nonextensive statistical mechanics [15], which has managed to describe a good number of phenomena ranging from optical phenomena such as anomalous transport in an optical lattice [16,17] to heavy-ion collisions [18,19]. Other applications of the Tsallis entropies involve recognizing that the parameter $\alpha = \frac{1}{2}$ is a natural operational measure of nonclassicality [20]. Another interesting measure of entanglement is logarithmic negativity [7], one of the most practical measures of quantifying mixed entanglement [21], which can be used as an upper bound on distillable entanglement [22] and has an unambiguous operational interpretation [23]. Furthermore, it allows a more varied selection of subsystems to be analyzed concerning entanglement with each other and through a medium. However, the logarithmic negativity is not convex, implying it can increase under mixing.

On the other hand, for some years, there have been attempts to construct classical analogs of quantum quantities, such as the Berry phase [24–26], linear quantum entropy [27], quantum geometric tensor [28–30], and more recently the quantum covariance matrix, purity, and von Neumann entropy [31]. These constructions have had the purpose of discovering to what extent quantum effects can be computed using classical mechanics tools and if these tools might shed some light on new properties of these quantum effects. In addition, these classical analogs aim to see if they can be more

*bodiazj@math.uc3m.es

†dgonzalezv@ipn.mx

‡mhm@ciencias.unam.mx

§vergara@nucleares.unam.mx

easily calculated than their quantum counterparts, at least in some particular cases. What has been discovered is that, in the case of Gaussian states, the classical analogs describe most of the quantum effects with remarkable accuracy, although some minor differences can be understood in terms of ordering anomalies [29]. In this article, we want to extend and compare these results in the framework of classical integrable systems by introducing classical analogs of the generalized purities, Rényi entropies, Bastiaans-Tsallis entropies, and logarithmic negativity. We shall see that this provides an alternative approach that effectively describes these other fundamental quantities of the quantum spectrum. Furthermore, some quantum mechanical systems have nonperturbative effects, which can be described with kinklike solutions [32], instantonlike solutions [33], flow tubes [34], domain walls [35], and others. The solution to these systems generally starts by obtaining an exact classical solution of a Euclidean version of the problem. So our idea of considering classical attack methods could give us information on a nonperturbative nature of a quantum system, which perhaps cannot be obtained by standard perturbative procedures.

The paper is organized as follows. In Sec. II, we fix the notation used throughout the paper and give a brief summary of the quantum purity, linear quantum entropy, and von Neumann entropy, as well as of their classical analogs for classical integrable systems introduced in [31]. We also include here an example that illustrates the use and main features of these classical analogs. In Sec. III, we review some basics about the generalized purities, Bastiaans-Tsallis, Rényi entropies, and logarithmic negativity. A key feature for our purposes is that these functions are entirely determined by the quantum covariance matrix if the system is in a Gaussian state. Then, taking this into account, in Sec. IV, we introduce classical analogs of generalized purities, Bastiaans-Tsallis entropies, Rényi entropies, and logarithmic negativity for classical integrable systems. Analogously to their quantum counterparts, these classical functions are completely determined by the classical covariance matrix of the classical integral system. In Sec. V, we provide three examples to illustrate the application of the introduced classical analogs, confronting the results with their quantum counterparts. The first example considers a system of linearly coupled harmonic oscillators, the second one a generalized harmonic oscillator chain, and the third one a one-dimensional circular lattice of oscillators. In all of these systems, the classical analogs agree with their quantum versions, for Gaussian states. Finally, in Sec. VI, we give our conclusions and some comments.

II. PRELIMINARIES

We begin by considering a quantum system described by a Hamiltonian $\hat{H}(\hat{\mathbf{q}}, \hat{\mathbf{p}})$ with a set of phase-space operators $\hat{\mathbf{q}} = \{\hat{q}_a\}$ and $\hat{\mathbf{p}} = \{\hat{p}_a\}$ ($a = 1, \dots, N$). We use bold letters with a hat to denote quantum operators. For a given quantum state $|m\rangle$, the quantum covariance matrix $\sigma = (\sigma_{\alpha\beta})$ is a $2N \times 2N$ matrix whose elements are

$$\sigma_{\alpha\beta} = \frac{1}{2} \langle \hat{\mathbf{r}}_\alpha \hat{\mathbf{r}}_\beta + \hat{\mathbf{r}}_\beta \hat{\mathbf{r}}_\alpha \rangle_m - \langle \hat{\mathbf{r}}_\alpha \rangle_m \langle \hat{\mathbf{r}}_\beta \rangle_m, \quad (1)$$

where $\hat{\mathbf{r}} = \{\hat{\mathbf{r}}_\alpha\} = (\hat{\mathbf{q}}_1, \dots, \hat{\mathbf{q}}_N, \hat{\mathbf{p}}_1, \dots, \hat{\mathbf{p}}_N)^\top$ ($\alpha, \beta = 1, \dots, 2N$) is a $2N$ -dimensional column vector and $\langle \hat{\mathbf{O}} \rangle_m = \langle m | \hat{\mathbf{O}} | m \rangle$

stands for the expectation value of an operator $\hat{\mathbf{O}}$. In the classical setting, the quantum covariance matrix has a counterpart for classical integrable systems [31]. Consider a classical integrable system defined by a Hamiltonian $H(q, p)$ with a set of canonical coordinates and momenta, $q = \{q^a\}$ and $p = \{p_a\}$ ($a = 1, \dots, N$). Within the Wigner function formalism, we consider the Wentzel-Kramers-Brillouin (WKB) approximation for the wave function $\psi_m(q) = \langle q | \psi_m \rangle$, which reads as

$$\psi_m(q) = \frac{1}{(2\pi)^{N/2}} \left| \det \frac{\partial^2 S(q, I_m)}{\partial q_a \partial I_b} \right|^{\frac{1}{2}} e^{\frac{i}{\hbar} S(q, I_m)}, \quad (2)$$

where $S(q, I_m)$ is the classical action corresponding to the particular torus I_m . Following Berry [36], we built the semiclassical Wigner function

$$W_m(q, p) = \frac{1}{(2\pi^2 \hbar)^N} \int dx e^{\frac{i}{\hbar} [S(q+x, I_m) - S(q-x, I_m) - 2px]} \times \left| \det \frac{\partial^2 S(q+x, I_m)}{\partial q_a \partial I_b} \det \frac{\partial^2 S(q-x, I_m)}{\partial q_a \partial I_b} \right|^{\frac{1}{2}}, \quad (3)$$

by considering a classical limit taking only linear corrections in the exponential and performing a canonical transformation of the phase-space coordinates to action-angle variables $I = \{I_a\}$ and $\varphi = \{\varphi_a\}$ ($a = 1, \dots, N$). In this case, the Wigner function of the system is reduced to a delta function

$$W_m(q, p) = \frac{1}{(2\pi)^N} \delta(I(q, p) - I_m), \quad (4)$$

involving only the action variables of the system and the value of the action corresponding to the m torus, i.e., $|\psi_m\rangle$, quantum state. We shall refer to this as the classical limit of the Wigner function. Furthermore, in this sense, we can identify our action variables with a constant.

Using this formalism it was shown in [31] that in the classical limit (which we denote by \simeq)

$$\sigma \simeq \sigma^{\text{cl}}, \quad (5)$$

where $\sigma^{\text{cl}} = (\sigma_{\alpha\beta}^{\text{cl}})$ is the classical covariance matrix with elements given by

$$\sigma_{\alpha\beta}^{\text{cl}} = \langle r_\alpha r_\beta \rangle_{\text{cl}} - \langle r_\alpha \rangle_{\text{cl}} \langle r_\beta \rangle_{\text{cl}}. \quad (6)$$

Here, $r = \{r_\alpha\} = (q_1, \dots, q_N, p_1, \dots, p_N)^\top$ is a phase-space column vector and

$$\langle f \rangle_{\text{cl}} = \frac{1}{(2\pi)^N} \int_0^{2\pi} \dots \int_0^{2\pi} d^N \varphi f, \quad (7)$$

with $d^N \varphi = d\varphi_1 \dots d\varphi_N$, is the classical average of a function $f = f(\varphi, I)$ over the angle variables.

The relation (5) was used in [31] to define classical analogs of some quantum quantities that serve as a measure of the mixedness of the quantum states and that for Gaussian states can be written as functions depending only on the quantum covariance matrix. Such quantities are the purity μ , linear quantum entropy S_L , and von Neumann entropy S which, for a normalized quantum state described by a density operator $\hat{\rho}$, are defined as [37,38]

$$\mu(\hat{\rho}) = \text{Tr} \hat{\rho}^2, \quad (8a)$$

$$S_L(\hat{\rho}) = 1 - \mu(\hat{\rho}), \tag{8b}$$

$$S(\hat{\rho}) = -\text{Tr}(\hat{\rho} \ln \hat{\rho}). \tag{8c}$$

For pure states $\hat{\rho}^2 = \hat{\rho}$, μ takes a maximum value of 1 and both entropies S_L and S are zero, whereas for mixed states, $\hat{\rho}^2 \neq \hat{\rho}$, these quantities vary in the range of $0 < \mu < 1$, $0 < S_L < 1$, and $S > 0$.

For a Gaussian state, the quantities (8) depend only on the corresponding quantum covariance matrix [37–46]. In fact, considering an n -mode Gaussian state (n denotes the degrees of freedom of the subsystem formed by the particles a_1, \dots, a_n of the system of N degrees of freedom) with the reduced quantum covariance matrix $\sigma_{(n)}$, we have

$$\mu(a_1, a_2, \dots, a_n) = \left(\frac{\hbar}{2}\right)^n \frac{1}{\sqrt{\det \sigma_{(n)}}} \tag{9a}$$

$$= \frac{1}{2^n} \prod_{k=1}^n v_k^{-1},$$

$$S_L(a_1, a_2, \dots, a_n) = 1 - \left(\frac{\hbar}{2}\right)^n \frac{1}{\sqrt{\det \sigma_{(n)}}}, \tag{9b}$$

$$S(a_1, a_2, \dots, a_n) = \sum_{k=1}^n S(v_k), \tag{9c}$$

where

$$S(v_k) = \left(v_k + \frac{1}{2}\right) \ln \left(v_k + \frac{1}{2}\right) - \left(v_k - \frac{1}{2}\right) \ln \left(v_k - \frac{1}{2}\right), \tag{10}$$

the subscript (n) represents (a_1, a_2, \dots, a_n) , and v_k are the symplectic eigenvalues of $\sigma_{(n)}/\hbar$, i.e., they are the entries of a non-negative diagonal matrix $\mathbf{D}_v = \text{diag}(v_1, \dots, v_n)$ which, together with a suitable symplectic matrix \mathbf{M} , allows us to write

$$\mathbf{M}^\top \left(\frac{\sigma_{(n)}}{\hbar}\right) \mathbf{M} = \begin{pmatrix} \mathbf{D}_v & \mathbf{0}_{n \times n} \\ \mathbf{0}_{n \times n} & \mathbf{D}_v \end{pmatrix}. \tag{11}$$

Notice that $S(v_k) = 0$ only if $v_k = \frac{1}{2}$, and that in the case $n = 1$, for the particle a_i , we have [40]

$$v_1 = \frac{1}{\hbar} \sqrt{\sigma_{\mathbf{p}_{a_i} \mathbf{p}_{a_i}} \sigma_{\mathbf{q}_{a_i} \mathbf{q}_{a_i}} - (\sigma_{\mathbf{q}_{a_i} \mathbf{p}_{a_i}})^2}. \tag{12}$$

Bearing in mind the relation (5) ($\sigma_{(n)} \simeq \sigma_{(n)}^{\text{cl}}$), the quantum functions (9), and the Bohr-Sommerfeld quantization rule for the action variables, in the sense $\hbar/2 \rightarrow I_k$, the *classical analogs* of the purity (9a), linear quantum entropy (9b), and von Neumann entropy (9c) are, respectively, defined as [31]

$$\tilde{\mu}^{\text{cl}}(a_1, a_2, \dots, a_n) := c_1^n \lim_{I_a \rightarrow c_1} \frac{1}{\sqrt{\det \sigma_{(n)}^{\text{cl}}}} \tag{13a}$$

$$= \left(\frac{1}{2^n}\right) \prod_{k=1}^n \tilde{\sigma}_k^{-1},$$

$$\tilde{S}_L^{\text{cl}}(a_1, a_2, \dots, a_n) := 1 - c_1^n \lim_{I_a \rightarrow c_1} \frac{1}{\sqrt{\det \sigma_{(n)}^{\text{cl}}}}, \tag{13b}$$

$$\tilde{S}^{\text{cl}}(a_1, a_2, \dots, a_n) := \sum_{k=1}^n S^{\text{cl}}(\tilde{\sigma}_k), \tag{13c}$$

where

$$S^{\text{cl}}(\tilde{\sigma}_k) := \left(\tilde{\sigma}_k + \frac{1}{2}\right) \ln \left(\tilde{\sigma}_k + \frac{1}{2}\right) - \left(\tilde{\sigma}_k - \frac{1}{2}\right) \ln \left(\tilde{\sigma}_k - \frac{1}{2}\right), \tag{14a}$$

$$\tilde{\sigma}_k := \frac{1}{2c_2} \lim_{I_a \rightarrow c_2} \sigma_k^{\text{cl}}, \tag{14b}$$

with σ_k^{cl} the symplectic eigenvalues of $\sigma_{(n)}^{\text{cl}}$, and I_{a_k} the action variables associated with the k -th normal mode. Note that $\tilde{\sigma}_k$ are the symplectic eigenvalues of $1/(2c_2) \lim_{I_a \rightarrow c_2} \sigma(n)^{\text{cl}}$ [analogous to v_k which are the symplectic eigenvalues of $\sigma(n)/\hbar$]. It is important to note that c_1 and c_2 are real positive constants that disappear during the calculation of quadratic Hamiltonian systems, which in the quantum context give rise to Gaussian states in their ground state. This is because, for these systems, the q and p variables depend linearly on the square root of I_k [see (17)]. Then, by identifying all I_k as c_2 , the classical covariance matrix becomes proportional to c_2 [see (19)], causing $\tilde{\sigma}_k$ to be independent of c_2 .

In the particular case of $n = 1$, for the particle a_i we get

$$\tilde{\sigma}_1 = \frac{1}{2c_2} \lim_{I_a \rightarrow c_2} \sqrt{\sigma_{\mathbf{p}_{a_i} \mathbf{p}_{a_i}}^{\text{cl}} \sigma_{\mathbf{q}_{a_i} \mathbf{q}_{a_i}}^{\text{cl}} - (\sigma_{\mathbf{q}_{a_i} \mathbf{p}_{a_i}}^{\text{cl}})^2}. \tag{15}$$

Notice that the limits in (13a) and (14b) involve not only a particular action variable I_{a_k} , but all the action variables.

We must note that to calculate the classical functions (13) no *a priori* knowledge of the corresponding quantum system is required. In addition, these functions are defined for any integrable system. However, it is only when the corresponding quantum system is in a Gaussian state that (13) are the classical analogs of the quantum purity, linear quantum entropy, and von Neumann entropy, respectively.

Example: Generalized harmonic oscillator chain

Let us now illustrate how to compute the classical analog of the purity. To this end let us take a generalized harmonic oscillator chain (GHOC) consisting of N coupled oscillators [47]. The Hamiltonian of the system is

$$H(q, p) = \frac{1}{2} p^\top p + \frac{1}{2} q^\top \mathbf{K} q + q^\top \mathbf{Y} p, \tag{16}$$

where $p = (p_1, \dots, p_N)^\top$, $q = (q_1, \dots, q_N)^\top$, \mathbf{Y} is an $N \times N$ diagonal matrix whose diagonal elements are parameters denoted by Y_a , and \mathbf{K} is $N \times N$ symmetric matrix of parameters.

Before starting we would like to make some general assertions about the stability of the system. We first determine the fixed points. The equations of motion coming from (16) are

$$\begin{pmatrix} \dot{q} \\ \dot{p} \end{pmatrix} = \mathbf{A} \begin{pmatrix} q \\ p \end{pmatrix}, \tag{17}$$

where

$$\mathbf{A} = \begin{pmatrix} \mathbf{Y} & \mathbf{1}_{N \times N} \\ -\mathbf{K} & -\mathbf{Y} \end{pmatrix}. \tag{18}$$

Setting $(\dot{q}, \dot{p}) = (0, 0)^\top$, it is direct to see that there is a unique fixed point at $(q^*, p^*)^\top = (0, 0)^\top$. To analyze the stability of this equilibrium point, we calculate the eigenvalues λ of the matrix \mathbf{A} . The characteristic equation for λ is $\det(\mathbf{M} + \lambda^2 \mathbf{1}) = 0$ where $\mathbf{M} := \mathbf{K} - \mathbf{Y}^2$. Then, denoting by ω_a^2 the eigenvalues of \mathbf{M} , the eigenvalues of the \mathbf{A} are $\lambda_a^{(\pm)} = \pm i\omega_a$. If we restrict

the system to $M > 0$, then ω_a are real and $\lambda_a^{(\pm)}$ are purely imaginary. This corresponds to a phase portrait of a center which is a stable system. On the other hand, if the matrix M is not positive semidefinite, we have at least one imaginary ω_a , and hence A has at least one positive and one negative eigenvalue, which originates an unstable hyperbolic system. Therefore, the condition $M > 0$ guarantees that the system is stable. In the following we consider $M > 0$.

To compute the classical analog of the purity, we start by performing the canonical transformation $q = q', p = p' - Yq$, followed by the canonical transformation of the form $Q = S^T q', P = S^T p'$, where S is such that it diagonalizes the matrix M , i.e., $SMS^T = \Omega^2$ where $\Omega = \text{diag}(\omega_1, \dots, \omega_N)$. Thus, the total canonical transformation can be written as $q = SQ$, $p = SP - YSQ$. In terms of the new variables (Q, P) the Hamiltonian (16) reads as

$$H(Q, P) = \frac{1}{2}P^T P + \frac{1}{2}Q^T \Omega^2 Q. \quad (19)$$

From (19) it is clear that ω_a are the normal frequencies of the system.

In terms of action-angle variables (I, ϕ) , the new variables (Q, P) can be written as $Q_a = \sqrt{\frac{2I_a}{\omega_a}} \sin \phi_a$, $P_a = \sqrt{2I_a \omega_a} \sin \phi_a$, and therefore

$$q_a = \sum_b S_{ab} \sqrt{\frac{2I_b}{\omega_b}} \sin \phi_b, \quad (20a)$$

$$p_a = \sum_b \left(S_{ab} \sqrt{2I_b \omega_b} \cos \phi_b - Y_a S_{ab} \sqrt{\frac{2I_b}{\omega_b}} \sin \phi_b \right). \quad (20b)$$

Using (7) and (20), the terms involved in the entries of the classical covariance matrix (6) are

$$\langle q_a q_b \rangle_{\text{cl}} = (S \mathbf{I} \Omega^{-1} S^T)_{ab}, \quad (21a)$$

$$\langle q_a p_b \rangle_{\text{cl}} = (S \mathbf{I} \Omega^{-1} S^T \mathbf{Y})_{ab}, \quad (21b)$$

$$\langle p_a p_b \rangle_{\text{cl}} = (S \mathbf{I} \Omega S^T + \mathbf{Y} S \mathbf{I} \Omega^{-1} S^T \mathbf{Y})_{ab}, \quad (21c)$$

$$\langle q_a \rangle_{\text{cl}} = \langle p_a \rangle_{\text{cl}} = 0, \quad (21d)$$

where $\mathbf{I} = \text{diag}(I_1, \dots, I_N)$. Notice that as a consequence of the term $q^T \mathbf{Y} p$ in the Hamiltonian (16), we have $\langle q_a p_b \rangle_{\text{cl}} \neq 0$ and the additional term $\mathbf{Y} S \mathbf{I} \Omega^{-1} S^T \mathbf{Y}$ in (21c). Considering that all action variables are equal to some constant c_1 , i.e., $I_a \rightarrow c_1$ for all $a = 1, \dots, N$, the classical covariance matrix takes the form

$$\lim_{I_a \rightarrow c_1} \sigma^{\text{cl}} = c_1 \begin{pmatrix} \mathbf{M}^{-1/2} & -\mathbf{M}^{-1/2} \mathbf{Y} \\ -\mathbf{Y} \mathbf{M}^{-1/2} & \mathbf{M}^{-1/2} + \mathbf{Y} \mathbf{M}^{-1/2} \mathbf{Y} \end{pmatrix}, \quad (22)$$

where $\mathbf{M}^{-1/2}$ is the inverse of the matrix $\mathbf{M}^{1/2} = S \Omega S^T$.

Using Schur complement is not hard to show that the determinant of (22) is c_1^{2N} , and then according to (13a), the classical analog of purity of the whole system is 1, which is the same result that follows from the quantum frame. In general, to compute the purity of a subsystem consisting of the first m ($m \leq N$) oscillators of the system, we need the associated reduced covariance matrix, which is obtained by taking the corresponding $m \times m$ block submatrix from (22).

The reduced covariance matrix $\sigma_{(m)}^{\text{cl}}$ can be written as

$$\sigma_{(m)}^{\text{cl}} = c_1 \begin{pmatrix} \mathbf{D} & -\mathbf{D} \mathbf{Y}_{\text{red}} \\ -\mathbf{Y}_{\text{red}} \mathbf{D} & \mathbf{A} + \mathbf{Y}_{\text{red}} \mathbf{D} \mathbf{Y}_{\text{red}} \end{pmatrix}, \quad (23)$$

where \mathbf{A} and \mathbf{D} are block matrices of $\mathbf{M}^{1/2}$ and $\mathbf{M}^{-1/2}$, respectively,

$$\mathbf{M}^{1/2} = \begin{pmatrix} \mathbf{A} & \mathbf{B} \\ \mathbf{B}^T & \mathbf{C} \end{pmatrix}, \quad (24a)$$

$$\mathbf{M}^{-1/2} = \begin{pmatrix} \mathbf{D} & \mathbf{E} \\ \mathbf{E}^T & \mathbf{F} \end{pmatrix}, \quad (24b)$$

and $\mathbf{Y}_{\text{red}} = \text{diag}(Y_1, \dots, Y_m)$.

Using (13a) and (23), the classical analog of purity of the m oscillators turns out to be

$$\tilde{\mu}^{\text{cl}}(a_1, \dots, a_m) = \frac{1}{\sqrt{\det \mathbf{A} \det \mathbf{D}}}, \quad (25)$$

where we have used Schur complement to simplify the determinant. Notice that even though the matrix \mathbf{Y}_{red} does not appear explicitly in this result, the classical analog of the purity depends on the parameters Y_a through the frequencies ω_a which are involved in \mathbf{A} and \mathbf{D} . We show below that this result is exactly the predicted one by the quantum purity (9a).

Before going to the quantum framework, we consider a particular case of (16) and provide an explicit expression for the classical analog of the purity. Let us take the system of two coupled generalized harmonic oscillators described by the Hamiltonian

$$H(q, p) = H_1 + H_2 + \frac{1}{2}Z(q_1 - q_2)^2, \quad (26)$$

where

$$H_a(q_a, p_a) = \frac{1}{2}[p_a^2 + Y_a(q_a p_a + p_a q_a) + X_a q_a^2]. \quad (27)$$

In this case, the matrices \mathbf{K} and \mathbf{M} are

$$\mathbf{K} = \begin{pmatrix} X_1 + Z & -Z \\ -Z & X_2 + Z \end{pmatrix}, \quad (28a)$$

$$\mathbf{M} = \begin{pmatrix} X_1 + Z - Y_1^2 & -Z \\ -Z & X_2 + Z - Y_2^2 \end{pmatrix}, \quad (28b)$$

and hence the matrix \mathbf{S} is

$$\mathbf{S} = \begin{pmatrix} \cos \theta & -\sin \theta \\ \sin \theta & \cos \theta \end{pmatrix}, \quad (29)$$

where $\tan \theta = \frac{\gamma}{|\gamma|}(\gamma^2 + 1) - \gamma$ with $\gamma := \frac{X_2 - X_1 + Y_1^2 - Y_2^2}{2Z}$. Here, we have considered $X_2 - X_1 + Y_1^2 - Y_2^2 \neq 0$ and $Z \neq 0$. Moreover, the normal frequencies are

$$\omega_1 = \sqrt{X_1 - Y_1^2 + Z - Z \tan \theta}, \quad (30a)$$

$$\omega_2 = \sqrt{X_2 - Y_2^2 + Z + Z \tan \theta}. \quad (30b)$$

Having these matrices at hand and using (21), we can compute the classical covariance matrix (22). The result is

$$\lim_{I_a \rightarrow c_1} \sigma^{\text{cl}} = \begin{pmatrix} \sigma_{qq}^{\text{cl}} & \sigma_{qp}^{\text{cl}} \\ \sigma_{pq}^{\text{cl}} & \sigma_{pp}^{\text{cl}} \end{pmatrix}, \quad (31)$$

where

$$\sigma_{qq}^{\text{cl}} = c_1 \begin{pmatrix} \frac{\cos^2 \theta}{\omega_1} + \frac{\sin^2 \theta}{\omega_2} & (\frac{1}{\omega_1} - \frac{1}{\omega_2}) \sin \theta \cos \theta \\ (\frac{1}{\omega_1} - \frac{1}{\omega_2}) \sin \theta \cos \theta & \frac{\sin^2 \theta}{\omega_1} + \frac{\cos^2 \theta}{\omega_2} \end{pmatrix}, \quad (32a)$$

$$\sigma_{qp}^{\text{cl}} = \sigma_{pq}^{\text{cl} \top} = c_1 \begin{pmatrix} Y_1 (\frac{\cos^2 \theta}{\omega_1} + \frac{\sin^2 \theta}{\omega_2}) & Y_2 (\frac{1}{\omega_1} - \frac{1}{\omega_2}) \sin \theta \cos \theta \\ Y_1 (\frac{1}{\omega_1} - \frac{1}{\omega_2}) \sin \theta \cos \theta & Y_2 (\frac{\sin^2 \theta}{\omega_1} + \frac{\cos^2 \theta}{\omega_2}) \end{pmatrix}, \quad (32b)$$

$$\sigma_{pp}^{\text{cl}} = c_1 \begin{pmatrix} \omega_1 \cos^2 \theta + \omega_2 \sin^2 \theta + Y_1^2 (\frac{\cos^2 \theta}{\omega_1} + \frac{\sin^2 \theta}{\omega_2}) & [(\omega_1 - \omega_2) + Y_1 Y_2 (\frac{1}{\omega_1} - \frac{1}{\omega_2})] \sin \theta \cos \theta \\ [(\omega_1 - \omega_2) + Y_1 Y_2 (\frac{1}{\omega_1} - \frac{1}{\omega_2})] \sin \theta \cos \theta & \omega_1 \sin^2 \theta + \omega_2 \cos^2 \theta + Y_2^2 (\frac{\sin^2 \theta}{\omega_1} + \frac{\cos^2 \theta}{\omega_2}) \end{pmatrix}. \quad (32c)$$

Using (25) together with (31), we find the classical analog of purity for a subsystem of one particle

$$\tilde{\mu}^{\text{cl}}(a_1) = \sqrt{\frac{\omega_1 \omega_2}{(\omega_1 \cos^2 \theta + \omega_2 \sin^2 \theta)(\omega_2 \cos^2 \theta + \omega_1 \sin^2 \theta)}}. \quad (33)$$

Notice that if $\omega_1 = \omega_2$, then (33) reduces to $\tilde{\mu}(a_1) = 1$. Nevertheless, in this case, γ is imaginary because of the condition $Z \neq 0$, i.e., since the oscillators are coupled. That γ is imaginary implies that the corresponding quantum Hamiltonian is non-Hermitian. The quantization of this type of systems has been done using PT symmetry [48,49], and it has been discovered that entanglement has different properties in this context [50,51]. In the general case $\omega_1 \neq \omega_2$, from (33) it follows that $\tilde{\mu}(a_1) < 1$ and hence the quantum counterpart of the system is entangled.

We now turn to the quantum framework. The quantum counterpart of the Hamiltonian (16) is

$$\hat{H}(\hat{q}, \hat{p}) = \frac{1}{2} \hat{p}^\top \hat{p} + \frac{1}{2} \hat{q}^\top K \hat{q} + \frac{1}{2} (\hat{q}^\top Y \hat{p} + \hat{p}^\top Y \hat{q}). \quad (34)$$

Performing a transformation analogous to the one that leads to (19), the Hamiltonian (34) can be diagonalized as $\hat{H}(\hat{Q}, \hat{P}) = \frac{1}{2} \hat{P}^\top \hat{P} + \frac{1}{2} \hat{Q}^\top \Omega^2 \hat{Q}$. To compute the components (1) of the quantum covariance matrix for the ground (Gaussian) state, it is convenient to write the operators \hat{Q} and \hat{P} as a combination of the usual raising and lowering operators. By doing this, the resulting quantum covariance matrix is the same as the classical covariance matrix (22), but with $\hbar/2$ replacing the constant c_1 . Using this result together with (9a), the quantum purity of the m quantum oscillators turns out to be equal to (25). This illustrates that the classical quantity $\tilde{\mu}^{\text{cl}}$ is capable of providing the same mathematical results as its quantum counterpart μ .

III. GENERALIZED PURITIES AND ENTROPIES, AND LOGARITHMIC NEGATIVITY

A. Generalized purities and entropies

The quantum quantities (8) can be generalized in the following sense: For a given quantum state $\hat{\rho}$, the generalized purities, Bastiaans-Tsallis entropies, and Rényi entropies [4]

for $\alpha \geq 0$ are given by [5,6,44,52]

$$\mu_\alpha(\hat{\rho}) = \text{Tr} \hat{\rho}^\alpha, \quad (35a)$$

$$S_\alpha(\hat{\rho}) = \frac{1 - \text{Tr} \hat{\rho}^\alpha}{\alpha - 1}, \quad (35b)$$

$$H_\alpha(\hat{\rho}) = \frac{\ln(\text{Tr} \hat{\rho}^\alpha)}{1 - \alpha}, \quad (35c)$$

respectively. Some comments regarding these generalizations. First, notice that $\text{Tr} \hat{\rho}^\alpha = (\|\hat{\rho}\|_\alpha)^\alpha$ where $\|\cdot\|_\alpha$ is the Schatten α -norm [44,53] and, in the asymptotic limit of arbitrary large α , $\text{Tr} \hat{\rho}^\alpha$ is a function of the largest eigenvalue of $\hat{\rho}$ only. Second, (35a) reduces to the purity (8a) when $\alpha = 2$. Third, for $\alpha = 2$, (35b) yields the linear entropy (8b), while in the limit $\alpha \rightarrow 1$ it reduces to the von Neumann entropy (8c). Fourth, in the limit $\alpha \rightarrow 1$, (35c) becomes the von Neumann entropy (8c). Fifth, in the limit $\alpha \rightarrow \infty$, S_α goes to a trivial constant null function, losing all information about the quantum state, while H_α converges to the min-entropy, which is the smallest entropy measure in the family of Rényi entropies [54,55]. Sixth, S_α is a monotonically decreasing function of α , for a given quantum state.

For a n -mode Gaussian state, associated with a subsystem formed by the particles a_1, \dots, a_n , (35) can be written as functions that only depend on the covariance matrix $\sigma_{(n)}$. In fact, they are given by [13,52,56]

$$\mu_\alpha(a_1, a_2, \dots, a_n) = \prod_{k=1}^n g_\alpha(v_k), \quad (36a)$$

$$S_\alpha(a_1, a_2, \dots, a_n) = \frac{1 - \prod_{k=1}^n g_\alpha(v_k)}{\alpha - 1}, \quad (36b)$$

$$H_\alpha(a_1, a_2, \dots, a_n) = \frac{\sum_{k=1}^n \ln [g_\alpha(v_k)]}{1 - \alpha}, \quad (36c)$$

where v_k are the symplectic eigenvalues of $\sigma_{(n)}/\hbar$, and

$$g_\alpha(v_k) = \frac{1}{(v_k + \frac{1}{2})^\alpha - (v_k - \frac{1}{2})^\alpha}. \quad (37)$$

Notice that $g_\alpha(\frac{1}{2}) = 1$ only if all eigenvalues satisfy $v_k = \frac{1}{2}$, which implies $\mu_\alpha = 1$, $S_\alpha = 0$, and $H_\alpha = 0$.

B. Logarithmic negativity

We now focus on the logarithmic negativity for a Gaussian state in a system of N coupled harmonic oscillators. We begin

by considering a set of $m = n_1 + n_2 \leq N$ oscillators that are divided into two groups: One of them with n_1 oscillators and another with n_2 oscillators. Assuming that there are no correlations between positions and momenta, the quantum covariant matrix associated with the m oscillators, which we refer to as the reduced covariance matrix $\boldsymbol{\mu}$, can be obtained from the quantum covariance matrix $\boldsymbol{\sigma}$ of the entire system by taking the rows and columns corresponding to the m oscillators. Then, under this condition, the matrix $\boldsymbol{\mu}$ has the form

$$\boldsymbol{\mu} = \frac{1}{2} \begin{pmatrix} \boldsymbol{\mu}_q & \mathbf{0}_{m \times m} \\ \mathbf{0}_{m \times m} & \boldsymbol{\mu}_p \end{pmatrix}, \quad (38)$$

where $\boldsymbol{\mu}_q$ and $\boldsymbol{\mu}_p$ are $m \times m$ matrices. Let us now consider the partial transpose $\boldsymbol{\mu}^\Gamma$ of $\boldsymbol{\mu}$ with respect to the group of n_2 oscillators, which is defined as

$$\boldsymbol{\mu}^\Gamma := \mathbf{P} \boldsymbol{\mu} \mathbf{P}, \quad (39)$$

where \mathbf{P} is a diagonal matrix given by

$$\mathbf{P} = \begin{pmatrix} \mathbf{1}_{m \times m} & \mathbf{0}_{m \times m} \\ \mathbf{0}_{m \times m} & \mathbf{P}_p \end{pmatrix}, \quad (40)$$

with $\mathbf{P}_p = \text{diag}(1, \dots, 1, -1, \dots, -1)$. The entries of \mathbf{P}_p are 1 for an oscillator of the group with n_1 oscillators or -1 for an oscillator belonging to the group with n_2 oscillators. It is not hard to verify that the effect of partial transposition with respect to the group of n_2 oscillators is to change the sign of the momenta corresponding to these oscillators.

To compute the logarithmic negativity we also require the symplectic matrix $\boldsymbol{\Omega} = (\Omega_{\alpha\beta})$, whose entries are given by

$$\Omega_{\alpha\beta} := -i[\hat{\mathbf{r}}_\alpha, \hat{\mathbf{r}}_\beta], \quad (41)$$

and has the block-matrix form

$$\boldsymbol{\Omega} = \hbar \begin{pmatrix} \mathbf{0}_{N \times N} & \mathbf{1}_{N \times N} \\ -\mathbf{1}_{N \times N} & \mathbf{0}_{N \times N} \end{pmatrix}. \quad (42)$$

Thus, for the set of m oscillators the associated symplectic matrix $\boldsymbol{\Sigma}$ takes the form

$$\boldsymbol{\Sigma} := \hbar \begin{pmatrix} \mathbf{0}_{m \times m} & \mathbf{1}_{m \times m} \\ -\mathbf{1}_{m \times m} & \mathbf{0}_{m \times m} \end{pmatrix}. \quad (43)$$

Using (39), (43), and considering the ground state of the chain, the logarithmic negativity $E_{\mathcal{N}}$, which provides a measure of entanglement between the two groups of n_1 and n_2 oscillators, is given by [7]

$$E_{\mathcal{N}} = - \sum_{k=1}^{2m} \log_2 [\min(1, |\lambda_k|)], \quad (44)$$

where λ_k ($k = 1, \dots, 2m$) are the eigenvalues of the matrix

$$\mathbf{B} = i \boldsymbol{\Sigma}^{-1} \boldsymbol{\mu}^\Gamma. \quad (45)$$

In fact, if $E_{\mathcal{N}}$ is positive, then the two groups of n_1 and n_2 oscillators are entangled. In terms of the matrices $\boldsymbol{\mu}_q$ and $\boldsymbol{\mu}_p$, the logarithmic negativity can be written as [23]

$$E_{\mathcal{N}} = - \sum_{j=1}^m \log_2 [\min(1, \tilde{\lambda}_j)], \quad (46)$$

where $\tilde{\lambda}_j$ are the eigenvalues of the matrix $\boldsymbol{\mu}_q \mathbf{P}_p \boldsymbol{\mu}_p \mathbf{P}_p / \hbar^2$.

Before concluding this section, it is worth pointing out that another useful measure of entanglement in composite systems is the *negativity* \mathcal{N} [7], which is related to the logarithmic negativity as

$$\mathcal{N} = \frac{2^{E_{\mathcal{N}}} - 1}{2}. \quad (47)$$

IV. CLASSICAL ANALOGS

A. Generalized purities and entropies

In this subsection, we define classical analogs of the generalized purities and entropies for Gaussian states (36) in the framework of classical integrable systems. We consider here a subsystem consisting of the n particles a_1, a_2, \dots, a_n of a classical integrable system of N degrees of freedom, which has been written in terms of the action-angle variables (φ, I) .

We start by introducing the classical analog of the function g_α for the subsystem (a_1, a_2, \dots, a_n) . Taking into account (37), the relation (5) for the quantum $\boldsymbol{\sigma}_{(n)}$ and classical $\boldsymbol{\sigma}_{(n)}^{\text{cl}}$ covariance matrices, i.e., $\boldsymbol{\sigma}_{(n)} \simeq \boldsymbol{\sigma}_{(n)}^{\text{cl}}$, and the Bohr-Sommerfeld quantization rule for the action variables, in the sense $\hbar/2 \rightarrow I_\alpha$, the classical analog of g_α is defined as

$$g_\alpha^{\text{cl}}(\tilde{\sigma}_k) := \frac{1}{(\tilde{\sigma}_k + \frac{1}{2})^\alpha - (\tilde{\sigma}_k - \frac{1}{2})^\alpha}, \quad (48)$$

where $\tilde{\sigma}_k$ is given by (14b). Notice that (48) can be obtained from (37) just by replacing the ν_i with $\tilde{\sigma}_k$, i.e., we are only changing the domain of the function, just as we did in the definition of the function \mathcal{S}^{cl} given by (14a).

With the help of the function g_α^{cl} , we define *classical analogs* of the generalized purities, Bastiaans-Tsallis entropies, and Rényi entropies for $\alpha \geq 0$ as

$$\tilde{\mu}_\alpha^{\text{cl}}(a_1, a_2, \dots, a_n) := \prod_{k=1}^n g_\alpha^{\text{cl}}(\tilde{\sigma}_k), \quad (49a)$$

$$\tilde{\mathcal{S}}_\alpha^{\text{cl}}(a_1, a_2, \dots, a_n) := \frac{1 - \prod_{k=1}^n g_\alpha^{\text{cl}}(\tilde{\sigma}_k)}{\alpha - 1}, \quad (49b)$$

$$\tilde{H}_\alpha^{\text{cl}}(a_1, a_2, \dots, a_n) := \frac{\sum_{k=1}^n \ln [g_\alpha^{\text{cl}}(\tilde{\sigma}_k)]}{1 - \alpha}, \quad (49c)$$

respectively. We point out that the functions (49) do not need to invoke any prior knowledge from the quantum framework, and as we will see through examples, they yield exactly the same mathematical results as their quantum counterparts. Also, notice that the functions (49) are defined for any integrable system, but only when the corresponding quantum system is in a Gaussian state they correspond to the classical analogs of the generalized purities, Bastiaans-Tsallis entropies, and Rényi entropies.

It is worth noticing that

$$\begin{aligned} \lim_{\alpha \rightarrow 1} \frac{\sum_{k=1}^n \ln [g_\alpha^{\text{cl}}(\tilde{\sigma}_k)]}{1 - \alpha} &= \lim_{\alpha \rightarrow 1} \frac{1 - \prod_{k=1}^n g_\alpha^{\text{cl}}(\tilde{\sigma}_k)}{\alpha - 1} \\ &= \sum_{k=1}^n \mathcal{S}^{\text{cl}}(\tilde{\sigma}_k), \end{aligned} \quad (50)$$

then

$$\begin{aligned} \lim_{\alpha \rightarrow 1} \tilde{S}_\alpha^{\text{cl}}(a_1, a_2, \dots, a_n) &= \lim_{\alpha \rightarrow 1} \tilde{H}_\alpha^{\text{cl}}(a_1, a_2, \dots, a_n) \\ &= \tilde{S}^{\text{cl}}(a_1, a_2, \dots, a_n), \end{aligned} \quad (51)$$

this is, in the limit $\alpha \rightarrow 1$ our classical analogs of the Bastiaans-Tsallis, $\tilde{S}_\alpha^{\text{cl}}$, and Rényi, $\tilde{H}_\alpha^{\text{cl}}$, entropies become the classical analog of the von Neumann entropy (13c), in complete analogy with the quantum case.

B. Logarithmic negativity for Gaussian states

To establish a classical analog of the logarithmic negativity (44) [or (46)], let us consider a classical integrable system of N coupled harmonic oscillators. As in the quantum case, we focus on a set of $m = n_1 + n_2 \leq N$ oscillators consisting of a group of n_1 oscillators and a group of n_2 oscillators. Furthermore, we also assume that there are no correlations between positions and momenta. Under these considerations, we begin by introducing the reduced classical covariance matrix μ^{cl} associated with the m oscillators, which subtracts the rows and columns corresponding to the m oscillators from the classical covariance matrix σ^{cl} . Then, the matrix μ^{cl} has the form

$$\mu^{\text{cl}} = \frac{1}{2} \begin{pmatrix} \mu_q^{\text{cl}} & \mathbf{0}_{m \times m} \\ \mathbf{0}_{m \times m} & \mu_p^{\text{cl}} \end{pmatrix}, \quad (52)$$

where μ_q^{cl} and μ_p^{cl} are $m \times m$ matrices. Also in this case we can define the partial transpose $(\mu^{\text{cl}})^\Gamma$ of μ^{cl} with respect to the group of n_2 oscillators, namely,

$$(\mu^{\text{cl}})^\Gamma := \mathbf{P} \mu^{\text{cl}} \mathbf{P}, \quad (53)$$

where \mathbf{P} is given by (40).

On the other hand, the classical analog of the symplectic matrix Ω , denoted by Ω^{cl} , can be obtained by replacing the commutator $[\cdot, \cdot]$ with the Poisson brackets $i\hbar\{\cdot, \cdot\}$. From this, we obtain the relation

$$\Omega \simeq \hbar \Omega^{\text{cl}}, \quad (54)$$

where $\Omega^{\text{cl}} = (\Omega_{\alpha\beta}^{\text{cl}})$ is the classical symplectic matrix and has entries given by

$$\Omega_{\alpha\beta}^{\text{cl}} := \{r_\alpha, r_\beta\}. \quad (55)$$

Using $\{q_a, p_b\} = \delta_{ab}$, it is not hard to realize that

$$\Omega^{\text{cl}} = \begin{pmatrix} \mathbf{0}_{N \times N} & \mathbf{1}_{N \times N} \\ -\mathbf{1}_{N \times N} & \mathbf{0}_{N \times N} \end{pmatrix}. \quad (56)$$

Hence, for the set of m oscillators the reduced classical symplectic matrix Σ^{cl} can be written as

$$\Sigma^{\text{cl}} = \begin{pmatrix} \mathbf{0}_{m \times m} & \mathbf{1}_{m \times m} \\ -\mathbf{1}_{m \times m} & \mathbf{0}_{m \times m} \end{pmatrix}. \quad (57)$$

Using (53) and (57), it is natural to define a classical analog of the logarithmic negativity (44) as

$$E_{\mathcal{N}}^{\text{cl}} = - \sum_{k=1}^{2m} \log_2 [\min(1, |\lambda_k^{\text{cl}}|)], \quad (58)$$

where λ_k^{cl} are the eigenvalues of the matrix

$$\mathbf{B}^{\text{cl}} = \frac{i}{2c_4} \lim_{I_a \rightarrow c_4} (\Sigma^{\text{cl}})^{-1} (\mu^{\text{cl}})^\Gamma. \quad (59)$$

Here, c_4 is an auxiliary real positive constant. Let us make some comments regarding (58). First, it is worth noticing that $E_{\mathcal{N}}^{\text{cl}}$ is a purely classical quantity since its definition does not require resorting to the quantum framework. Second, the (arbitrary) constant c_4 disappears from (59) once the limit $I_a \rightarrow c_4$ is taken, and therefore $E_{\mathcal{N}}^{\text{cl}}$ does not depend on this constant. Third, by following a procedure completely analogous to the one leading to (46) (see Ref. [23]), the classical analog of the logarithmic negativity can be written in terms of μ_q^{cl} and μ_p^{cl} as

$$E_{\mathcal{N}}^{\text{cl}} = - \sum_{j=1}^m \log_2 [\min(1, \tilde{\lambda}_j^{\text{cl}})], \quad (60)$$

where $\tilde{\lambda}_j^{\text{cl}}$ are the eigenvalues of the matrix

$$\tilde{\mathbf{B}}^{\text{cl}} = \frac{1}{(2c_4)^2} \lim_{I_a \rightarrow c_4} \mu_q^{\text{cl}} \mathbf{P}_P \mu_p^{\text{cl}} \mathbf{P}_P. \quad (61)$$

Note that using $E_{\mathcal{N}}^{\text{cl}}$ we can also introduce a classical analog of the negativity \mathcal{N} . Bearing in mind Eq. (47), we define a classical analog of the negativity as

$$\mathcal{N}^{\text{cl}} = \frac{2^{E_{\mathcal{N}}^{\text{cl}}} - 1}{2}. \quad (62)$$

Since \mathcal{N}^{cl} is trivially related to $E_{\mathcal{N}}^{\text{cl}}$, in the next section we only present numerical checks of $E_{\mathcal{N}}^{\text{cl}}$.

V. EXAMPLES

In this section, we present some examples to illustrate the application of the proposed classical functions. In Sec. V A, we compute the classical analogs of the generalized purities, Bastiaans-Tsallis entropies, and Rényi entropies for a linearly coupled harmonic oscillator system, and compare them with their quantum counterparts for the ground state of the system. In Sec. V B, we consider the particular case of the generalized harmonic oscillator chain given by the Hamiltonian (26) and compare the generalized purities and entropies with their classical analogs. Finally, in Sec. V C, for a circular lattice of oscillators in several configurations, we compute the classical analog of the logarithmic negativity (58) and compare it with its quantum counterpart.

We will see in these examples that our classical approach provides exactly the same results as their quantum counterparts when the quantum counterpart of the system is in a Gaussian state.

A. Linearly coupled harmonic oscillators

Let us consider the system composed of two coupled harmonic oscillators described by the Hamiltonian

$$H(q, p) = \frac{1}{2}(p_1^2 + p_2^2 + Aq_1^2 + Bq_2^2 + Cq_1q_2), \quad (63)$$

where A , B , and C are real parameters such that $A, B > 0$, $A \neq B$, and $4AB - C^2 \geq 0$. This system has been widely used for the analysis of quantum entanglement [57,58], and one

of its features is that it presents a very large quantum entanglement for certain parameter values [2,59,60]. Recently, in [31] this system was also used to study the classical analogs of purity, linear quantum entropy, and von Neumann entropy, finding that these classical functions provide the same results as their quantum counterparts. Furthermore, this model was

used to study the classical analog of the quantum geometric tensor [29]. Interestingly and in contrast to the classical functions studied in [31], it was shown that the classical metric tensor does not yield the full parameter structure of its quantum counterpart, the cause being a quantum ordering anomaly.

Using the corresponding action-angle variables (φ_a, I_a) ($a = 1, 2$), the components of the classical covariance matrix σ^{cl} of the system are [31]

$$\sigma_{qq}^{\text{cl}} = \begin{pmatrix} \frac{I_1 \cos^2 \beta}{\omega_1} + \frac{I_2 \sin^2 \beta}{\omega_2} & (\frac{I_2}{\omega_2} - \frac{I_1}{\omega_1}) \sin \beta \cos \beta \\ (\frac{I_2}{\omega_2} - \frac{I_1}{\omega_1}) \sin \beta \cos \beta & \frac{I_1 \sin^2 \beta}{\omega_1} + \frac{I_2 \cos^2 \beta}{\omega_2} \end{pmatrix}, \quad (64a)$$

$$\sigma_{pp}^{\text{cl}} = \begin{pmatrix} I_1 \omega_1 \cos^2 \beta + I_2 \omega_2 \sin^2 \beta & (I_2 \omega_2 - I_1 \omega_1) \sin \beta \cos \beta \\ (I_2 \omega_2 - I_1 \omega_1) \sin \beta \cos \beta & I_1 \omega_1 \sin^2 \beta + I_2 \omega_2 \cos^2 \beta \end{pmatrix}, \quad (64b)$$

$$\sigma_{qp}^{\text{cl}} = \mathbf{0}_{2 \times 2}, \quad (64c)$$

where ω_1 and ω_2 are the normal frequencies

$$\omega_1 := \sqrt{A - \frac{C}{2} \tan \beta}, \quad \omega_2 := \sqrt{B + \frac{C}{2} \tan \beta}, \quad (65)$$

and $\tan 2\beta = C/(B - A)$ with $\beta \in (-\pi/4, \pi/4)$.

In this case, the subsystems are each oscillator {1} and {2}; and the complete system {1,2}. For the subsystem {1} the corresponding $\tilde{\sigma}_1$ [see (14b)] is

$$\tilde{\sigma}_1 = \frac{1}{2} \sqrt{\left(\frac{\cos^2 \beta}{\omega_1} + \frac{\sin^2 \beta}{\omega_2} \right) (\omega_1 \cos^2 \beta + \omega_2 \sin^2 \beta)}, \quad (66)$$

which in terms of the original parameters reduces to

$$\tilde{\sigma}_1 = \sqrt{\frac{AB}{4AB - C^2}}, \quad (67)$$

and, because of the symmetry between the subsystems {1} and {2}, the symplectic eigenvalue of the subsystem {2} satisfies $\tilde{\sigma}_2 = \tilde{\sigma}_1$. Notice that in the uncoupled regime $C = 0$, $\tilde{\sigma}_1 = \tilde{\sigma}_2 = \frac{1}{2}$ and then the classic analogs of the generalized purities and entropies are 1 and 0 for all $\alpha > 1$, respectively, which means that the oscillators are separated in phase space. Furthermore, the symplectic eigenvalues of the complete system {1, 2} are $\sigma_1 = \frac{1}{2} = \sigma_2 = \tilde{\sigma}_1 = \tilde{\sigma}_2$, which means that the complete system is pure as expected.

Using (49) and (67), we compute the classical analogs of the generalized purities and entropies defined by (49) for $\alpha \rightarrow 1$ and $\alpha = 0.9, 2, 4, 8, 16, 32, 64$. Also, for illustrative purposes, we set $AB = 100$. In Fig. 1 we show the numerical results of the classical analogs as functions of the coupling constant C , which with the election $AB = 100$ can take values in the interval $(-20, 20)$. As these functions are symmetric under $C \rightarrow -C$, we only plot the region $[0, 20)$. Let us make some comments about it: (i) These plots illustrate what we have said about the case $C = 0$. (ii) We have included the case $\alpha = 2$, then Fig. 1(a) contains the analog of the purity. (iii) We have included in Figs. 1(b) and 1(c) the limit $\alpha \rightarrow 1$, which corresponds with the von Neumann entropy, given by

$$\tilde{S}^{\text{cl}}(1) = \left(\sqrt{\frac{AB}{4AB - C^2}} + \frac{1}{2} \right) \ln \left(\sqrt{\frac{AB}{4AB - C^2}} + \frac{1}{2} \right) - \left(\sqrt{\frac{AB}{4AB - C^2}} - \frac{1}{2} \right) \ln \left(\sqrt{\frac{AB}{4AB - C^2}} - \frac{1}{2} \right) = \tilde{S}^{\text{cl}}(2), \quad (68a)$$

$$\tilde{S}^{\text{cl}}(1, 2) = 0. \quad (68b)$$

This classical analog was discussed in [31]. (iv) In Figs. 1(b) and 1(c) we inset subfigures to illustrate the global behavior of the classical analogs of the generalized entropies. (v) We can appreciate some general characteristics of the generalized entropies; for instance, in Fig. 1(b) we observe that Tsallis entropies are monotonically decreasing functions of α and Fig. 1(c) shows the concave behavior of Rényi entropies.

Let us now consider the quantum case. Using the quantum counterpart of the Hamiltonian (63), the components of the quantum covariance matrix σ for the ground state are

$$\sigma_{qq} = \frac{\hbar}{2} \begin{pmatrix} \frac{\cos^2 \beta}{\omega_1} + \frac{\sin^2 \beta}{\omega_2} & (\frac{1}{\omega_2} - \frac{1}{\omega_1}) \sin \beta \cos \beta \\ (\frac{1}{\omega_2} - \frac{1}{\omega_1}) \sin \beta \cos \beta & \frac{\sin^2 \beta}{\omega_1} + \frac{\cos^2 \beta}{\omega_2} \end{pmatrix}, \tag{69a}$$

$$\sigma_{pp} = \frac{\hbar}{2} \begin{pmatrix} \omega_1 \cos^2 \beta + \omega_2 \sin^2 \beta & (\omega_2 - \omega_1) \sin \beta \cos \beta \\ (\omega_2 - \omega_1) \sin \beta \cos \beta & \omega_1 \sin^2 \beta + \omega_2 \cos^2 \beta \end{pmatrix}, \tag{69b}$$

$$\sigma_{qp} = \mathbf{0}_{2 \times 2}. \tag{69c}$$

Bearing in mind the Bohr-Sommerfeld quantization rule $I_a \rightarrow \hbar/2$, it is direct to show that the resulting classical and quantum covariant matrices (64) and (69) are exactly the same. Therefore, the resulting generalized purities and entropies (36) of the subsystems are the same as determined from the classical functions (49). This corroborates that our classical analogs are capable of giving rise to the same mathematical results as their quantum versions.

B. Generalized harmonic oscillator chain

In this section, we continue with the example of a generalized harmonic oscillator chain, whose Hamiltonian is presented in (26). For this system, we have already computed the classical covariance matrix and the classical analog of the purity. Now we will focus on the classical analogs of generalized purities, Bastiaans-Tsallis, and Rényi entropies, which can be calculated by using (49) and the symplectic eigenvalues of the reduced covariance matrix (32). The symplectic eigenvalues have the same functional form of (66), but with normal frequencies given by (30). The resulting expressions for these classical quantities will not be given explicitly, but instead, we plot them for $\alpha = 0.9, 2, 4, 8, 16, 32, 64$ and $\alpha \rightarrow 1$, as functions of the parameter Y_2 . We fix the rest of the parameters as $X_1 = X_2 = 2, Z = 1$, and $Y_1 = 0$. This choice implies that Y_2 can take values in the interval $(-\sqrt{8/3}, \sqrt{8/3})$ (out of this interval the normal frequencies have an imaginary part). As these functions are symmetric under $Y_2 \rightarrow -Y_2$ we only plot the region $[0, \sqrt{8/3})$. The results are shown in Fig. 2. Notice that the classical analogs of Rényi entropies are always concave [see Fig. 2(c)], while the corresponding analogs of Bastiaans-Tsallis entropies are not [see Fig. 2(b)]. On one hand, for $\alpha > 1$, in the limit $Y_2 \rightarrow \sqrt{8/3}$ the classical analogs of generalized purities go to zero [see Fig. 2(a)], while the classical analogs of Rényi entropies diverge and the classical analogs of Bastiaans-Tsallis entropies go to $1/(\alpha - 1)$. On the other hand, for $0 < \alpha \leq 1$ and $Y_2 \rightarrow \sqrt{8/3}$, the classical analogs of both Rényi and Bastiaans-Tsallis entropies diverge. Remarkably, we find that all these results (obtained by classical methods) coincide with those obtained by the quantum approach.

C. One-dimensional circular lattice of oscillators

To close this section, we want to present numerical checks of our classical analog of the logarithmic negativity (60) for two groups of n_1 and n_2 oscillators in a system of N identical oscillators on a one-dimensional circular lattice. The

Hamiltonian of the system under consideration is

$$H = \frac{1}{2} \sum_{a=1}^N [p_a^2 + kq_a^2 + \kappa(q_a - q_{a+1})^2], \tag{70}$$

with the periodic boundary condition $q_1 \equiv q_{N+1}$. This system has been investigated in the context of logarithmic negativity [23,61,62], entanglement between collective operators [63], and circuit complexity [64]. It is worth noting that the Hamiltonian (70) is a particular case of the Hamiltonian (16), i.e., the case where $Y = 0$ and K is an $N \times N$ symmetric circulant matrix given by

$$K = \begin{pmatrix} k + 2\kappa & -\kappa & 0 & \dots & -\kappa \\ -\kappa & k + 2\kappa & -\kappa & \dots & 0 \\ 0 & -\kappa & \ddots & \ddots & \vdots \\ \vdots & \vdots & \ddots & \ddots & -\kappa \\ -\kappa & 0 & \dots & -\kappa & k + 2\kappa \end{pmatrix}. \tag{71}$$

This matrix is orthogonally diagonalizable and then can be expressed as $K = U^T \Omega^2 U$, where U is an orthogonal matrix and $\Omega = \text{diag}(\omega_1, \dots, \omega_N)$ with $\omega_1, \dots, \omega_N$ being the normal frequencies of the system.

To study the classical analog of the logarithmic negativity, we now consider a set of $m = n_1 + n_2 \leq N$ oscillators consisting of two groups of n_1 and n_2 oscillators. In this case, the reduced $2m \times 2m$ classical covariance matrix μ^{cl} for the set of m oscillators is obtained directly from the $2N \times 2N$ classical covariance matrix σ^{cl} of the system,

$$\sigma^{\text{cl}} = \begin{pmatrix} U^T \Omega^{-1} I U & \mathbf{0}_{N \times N} \\ \mathbf{0}_{N \times N} & U^T \Omega I U \end{pmatrix}, \tag{72}$$

by subtracting the corresponding rows and columns of the m oscillators. Here, $I = \text{diag}(I_1, \dots, I_N)$ is a diagonal matrix whose elements are the action variables I_a . From the resulting matrix μ^{cl} we can read off the matrices μ_q^{cl} and μ_p^{cl} and then construct the matrix \tilde{B}^{cl} given by (61) for each considered case. It is important to point out that the resulting matrix \tilde{B}^{cl} does not depend on the auxiliary constant c_4 , despite the fact that its construction involves such a constant. Having \tilde{B}^{cl} , we find the classical logarithmic negativity (60) by a simple numerical calculation.

Let us begin by considering a system of $N = 200$ oscillators which involves two disjoint groups of $n_1 = 50$ and $n_2 = 50$ oscillators, separated by d oscillators. The oscillators 51 to

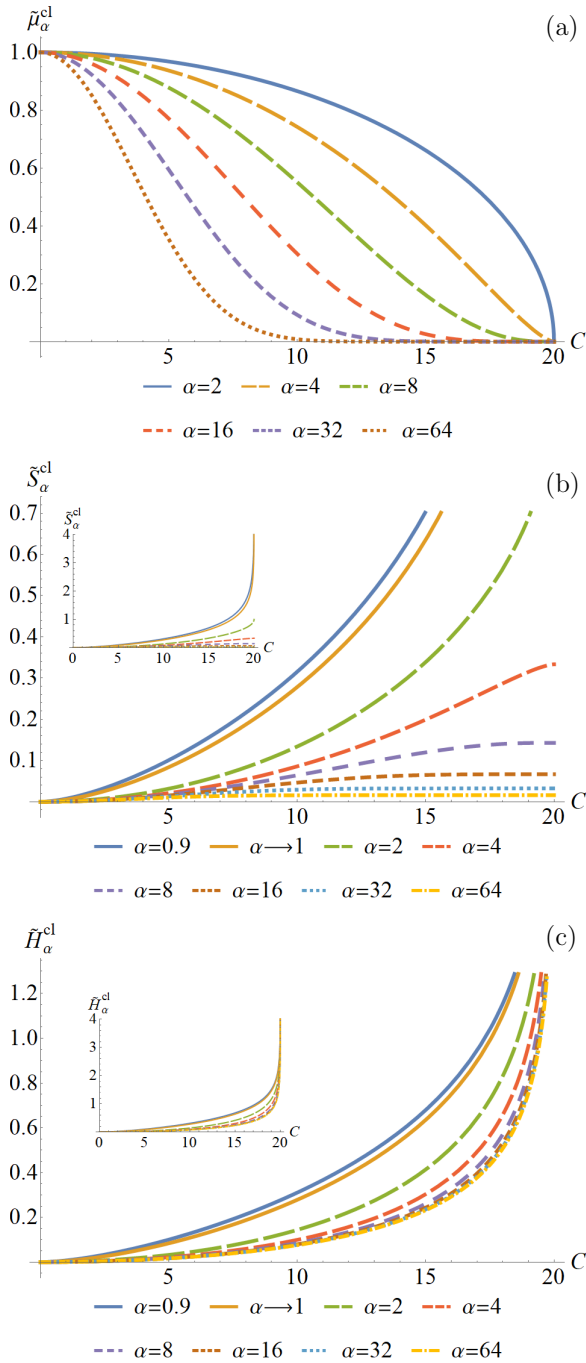


FIG. 1. Plots of the classical analogs, as a function of C for different values of α , for (a) generalized purities, (b) Bastiaans-Tsallis, and (c) Rényi entropies.

$50 + d$ and $101 + d$ to 200 are not part of the two groups. In Fig. 3, we show an illustration of this setup.

In Fig. 4(a), we plot the classical analog of the logarithmic negativity, on a logarithmic scale, as a function of d and the coupling constant κ , with $k = 0.1$. From this figure we see that, given a value of κ , the classical analog of the logarithmic takes a maximum value at $d = 0$ and 100 , whereas it takes a minimum value when $d = 50$ which corresponds to the most symmetric case. This can be better appreciated in Fig. 4(b) where we plot the classical analog of the logarithmic

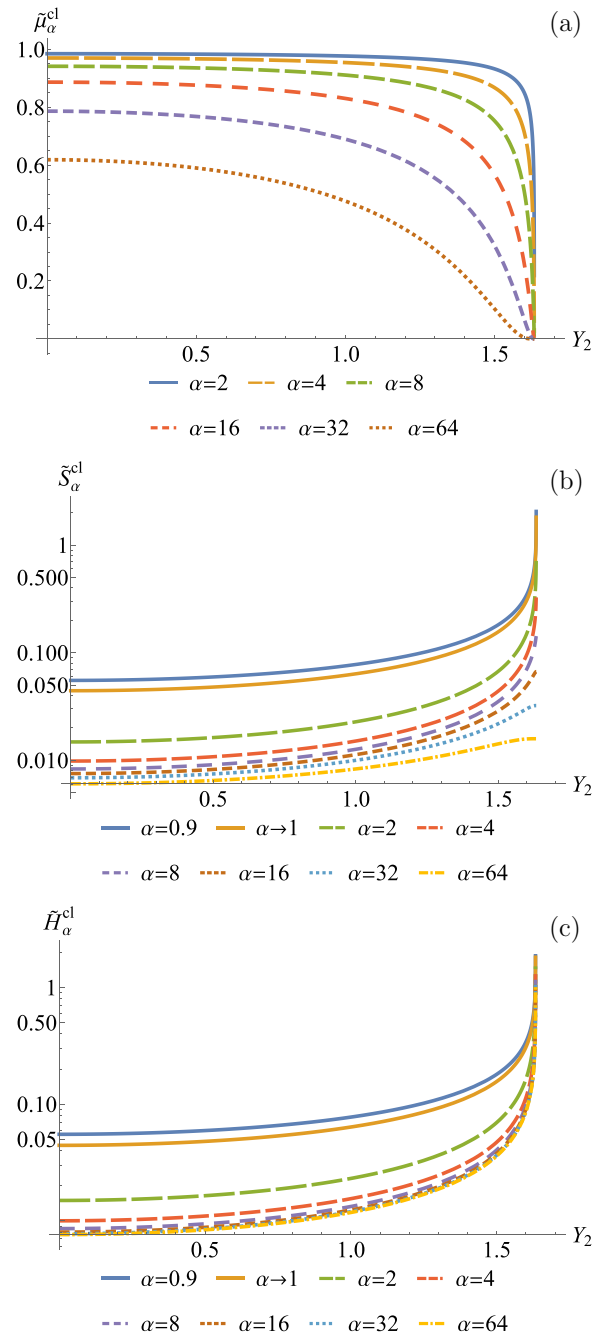


FIG. 2. Plots of the classical analogs, as a function of Y_2 for different values of α , for (a) generalized purities, (b) Bastiaans-Tsallis, and (c) Rényi entropies.

negativity, on a logarithmic scale, as a function of d for some values of κ . In this plot, we can also see that $E_{\mathcal{N}}^{\text{cl}}$ decreases from $d = 0$ to 50 following a near-exponential form. This result is in agreement with the one reported in [23] for the effect of the group separation on the logarithmic negativity. Notice that due to the symmetry of the setup, $E_{\mathcal{N}}^{\text{cl}}$ increases from $d = 50$ to 100 following a near-exponential form. Another feature that we can see is that the minimum values of $E_{\mathcal{N}}^{\text{cl}}$ (at $d = 50$) increase as κ increases. From Fig. 4(c) we can see the behavior of the classical analog of the logarithmic negativity with respect to κ , for different values of d . Here

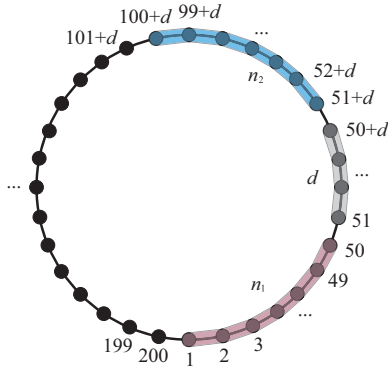


FIG. 3. Illustration of the setup used in the first case. Two disjoint groups of $n_1 = 50$ and $n_2 = 50$ oscillators of a circular lattice of $N = 200$ oscillators. The groups are separated by d oscillators

we see that E_N^{cl} increases as κ increases, which is an expected result. It can be verified that these results coming from the classical analog of the logarithmic negativity are exactly the same as those obtained using logarithmic negativity given by Eq. (46).

Let us now illustrate our approach on a system with two adjacent ($d = 0$) groups of $n_1 \leq 100$ and $n_2 = 100 - n_1$ oscillators in a circular lattice of $N = 200$ oscillators. Note that in general the groups have different sizes ($n_1 \neq n_2$) while the set has a fixed size ($m = n_1 + n_2 = 100$) and that the oscillators 101 to 200 are not part of the two groups. The setup is depicted in Fig. 5. In this case, we fix $k = 0.0001$.

The numerical calculation yields the results depicted in Fig. 6(a), where we show a map of the classical analog of the logarithmic negativity as a function of κ and n_1 . Note that when n_1 is kept fixed the classical function E_N^{cl} increases with κ . This behavior can be seen more clearly in Fig. 6(b), which also shows that the value of E_N^{cl} for $n_1 = 50$ ($n_1 = n_2$) is greater than the corresponding values for $n_1 \neq 50$ ($n_1 \neq n_2$). In Fig. 6(c), we plot the classical analog of the logarithmic negativity as a function of n_1 for $\kappa = 2, 64$. We see that the lowest value of E_N^{cl} is obtained for $n_1 = 0$ ($n_2 = 100$) and $n_1 = 100$ ($n_2 = 0$), while the highest value of E_N^{cl} is obtained for the symmetric configuration $n_1 = 50$ ($n_2 = 50$). This effect of the group sizes n_1 and n_2 on E_N^{cl} is analogous to the one found in [23] for asymmetrically bisected chains, in the sense that the value of E_N^{cl} with $n_1 = n_2$ provides an upper bound on the values with $n_1 \neq n_2$. On the other hand, the logarithmic negativity for two adjacent intervals of lengths n_1, n_2 of a finite system of length N is given by [61,62]

$$E_N = \frac{b_1}{4} \ln \left[\frac{N \sin\left(\frac{\pi n_1}{N}\right) \sin\left(\frac{\pi n_2}{N}\right)}{\pi \sin\left(\frac{\pi(n_1+n_2)}{N}\right)} \right] + b_2, \quad (73)$$

where b_1 and b_2 are constants. Plugging $N = 200$ and $n_2 = 100 - n_1$ into this expression, the logarithmic negativity reduces to

$$E_N = \frac{b_1}{4} \ln \left[\frac{100}{\pi} \sin\left(\frac{\pi n_1}{100}\right) \right] + b_2. \quad (74)$$

In Fig. 6(c), we also plot E_N given by (74) as a function of n_1 with $b_1 = 2.5834$, $b_2 = 1.3864$ (blue continuous

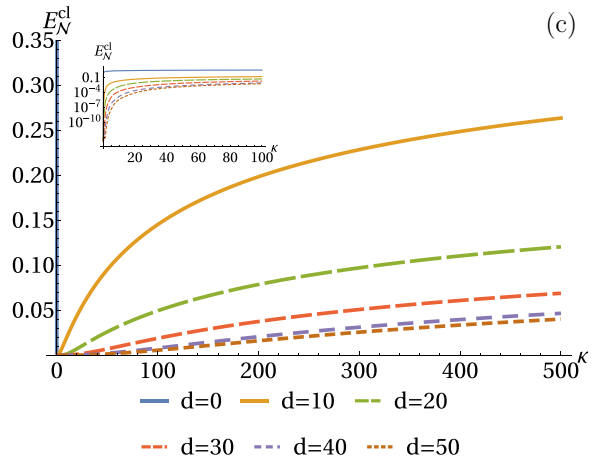
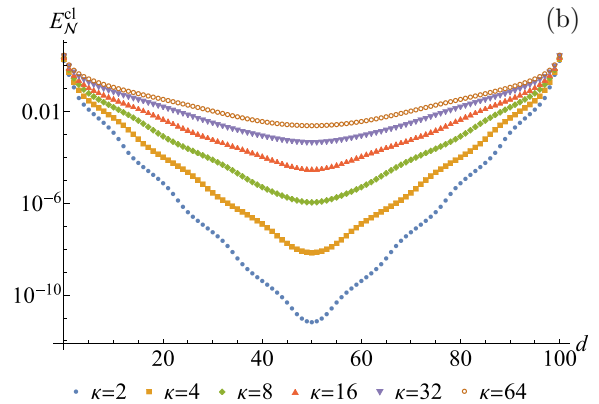
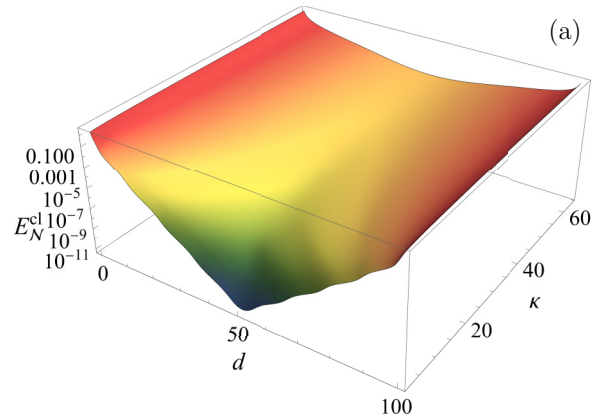


FIG. 4. Classical analog of the logarithmic negativity for two groups of $n_1 = n_2 = 50$ oscillators embedded in a harmonic chain of $N = 200$ oscillators with $k = 0.1$. d is the number of oscillators between the two groups, as shown in Fig. 3.

line) and $b_1 = 2.7464$, $b_2 = 1.3448$ (orange continuous line), which fit well to the data for $\kappa = 4$ and 64 , respectively. This corroborates the predictions made by our classical approach. Furthermore, we verify that the numerical results obtained in this case using the classical function E_N^{cl} are the same as those determined with the logarithmic negativity E_N . It is interesting to note that, in the quantum context, b_1 in (74) (or (73)) is associated with the central charge which can be regarded as a measure of the degrees of freedom of a system. Of course, the notion of central charge only makes sense in our chain of oscillators (70) in the conformal limit, i.e., when

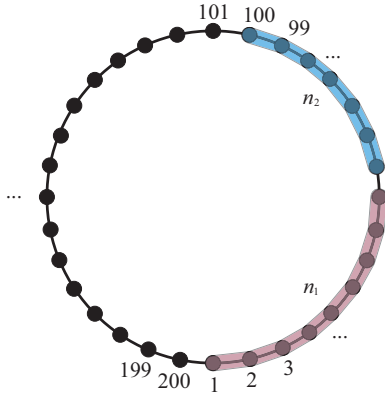


FIG. 5. Illustration of the setup considered in the second case. Two adjacent groups of n_1 and $n_2 = 100 - n_1$ oscillators of a circular lattice of $N = 200$ oscillators.

the constant k goes to zero. As we are considering $k = 0.0001$ this approaches the aforementioned limit. This means that the values of b_1 obtained by following our classical approach can be regarded as an estimation of the central charge since in this case, $E_{\mathcal{N}}^{\text{cl}}$ leads to the same results as its quantum counterpart. Nevertheless, understanding the role of the constant b_1 in the classical framework requires further analysis.

Finally, the third case is devoted to studying two adjacent groups of equal sizes $n_1 = n_2 = 10$ embedded in a harmonic chain of N oscillators. The setup is illustrated in Fig. 7, where it is also clear that the oscillators 21 to N do not belong to the two groups.

In Fig. 8(a), we show the numerical results for the classical analog of the logarithmic negativity as a function of N and κ . From this plot, we see two features. First, $E_{\mathcal{N}}^{\text{cl}}$ increases with κ , which also happened in the two previous cases and is expected. Second, for a fixed value of κ , $E_{\mathcal{N}}^{\text{cl}}$ decreases as N increases and asymptotically approaches a finite constant value for large N . This behavior is shown explicitly in Fig. 8(b) for different values of the coupling constant κ . Moreover, from this plot, we can see that there is a dependence on κ of the value to which $E_{\mathcal{N}}^{\text{cl}}$ approaches.

To gain more insight into this, in Fig. 9 we show $E_{\mathcal{N}}^{\text{cl}}$ as a function of κ for a fixed system size of $N = 500$ oscillators, which in this case is large enough to avoid finite-size effects [see Fig. 8(b)]. We see that, for large N , $E_{\mathcal{N}}^{\text{cl}}$ increases as κ increases and behaves as

$$E_{\mathcal{N}}^{\text{cl}} \sim 2.458 - \frac{2.149}{\kappa^{0.641} + 0.875}. \quad (75)$$

To conclude this case, we point out that the results reported in Figs. 8 and 9 are exactly the same as those given by the logarithmic negativity. Thus, our results in the three considered cases corroborate that, in fact, $E_{\mathcal{N}}^{\text{cl}}$ can be regarded as a classical analog of the logarithmic negativity for a Gaussian state in a system of N coupled harmonic oscillators.

VI. CONCLUSIONS

In this article, we consider classical integrable systems and introduce four new classical analogs of quantum

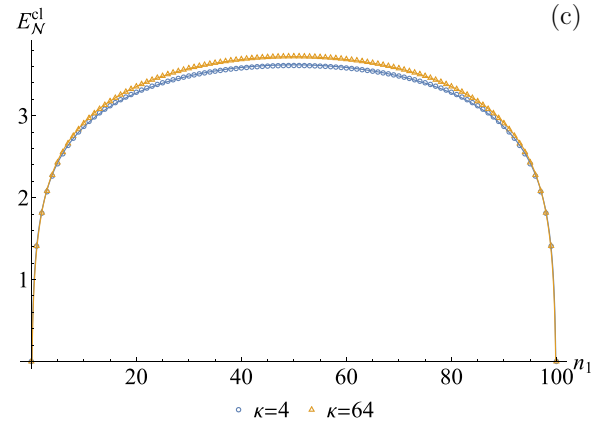
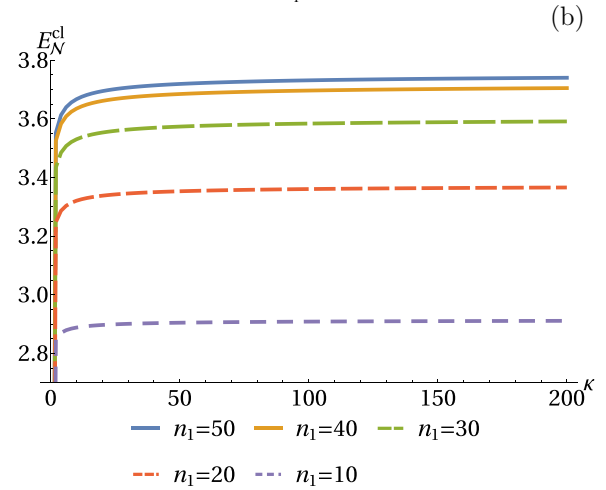
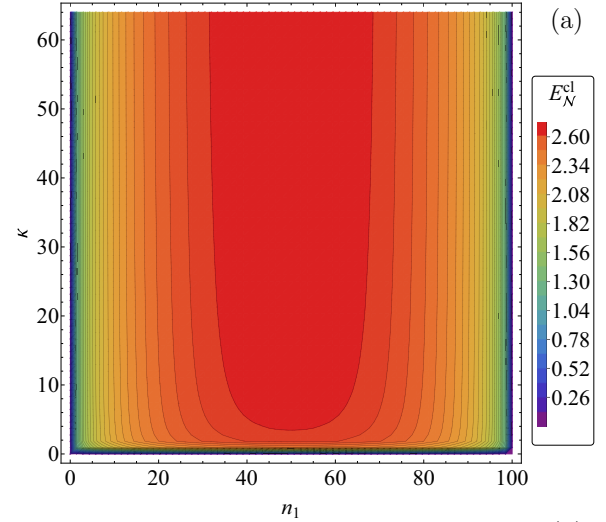


FIG. 6. Classical analog of the logarithmic negativity for two adjacent groups of sizes n_1 and $n_2 = 100 - n_1$ in a harmonic chain of $N = 200$ oscillators with $k = 0.0001$. Continuous lines in (c) are the fit obtained with (74).

quantities that measure entanglement: Generalized purities, Rényi entropies, Bastiaans-Tsallis entropies, and logarithmic negativity. These classical analogs involve an identification of all the action variables of the classical system with a real positive constant, which disappears at the end of the computation. We show through examples that all these classical analogs

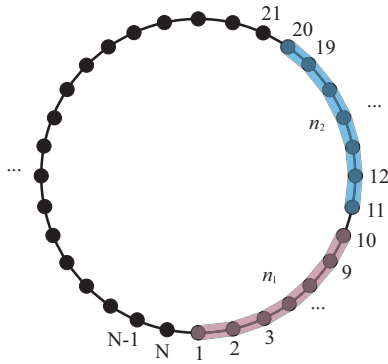


FIG. 7. Illustration of the setup used in the third case. Two adjacent groups of $n_1 = 10$ and $n_2 = 10$ oscillators of a circular lattice of N oscillators.

exactly reproduce the quantum results in the case of Gaussian states. For non-Gaussian states, the results are not reproduced essentially because the covariance matrix does not entirely determine these states.

In the case of linearly coupled harmonic oscillators, from our results in Sec. V, we observe that the generalized purities are more sensitive than the generalized entropies to the change in the coupling constant of the oscillators, which could be of interest from an experimental point of view. On the other

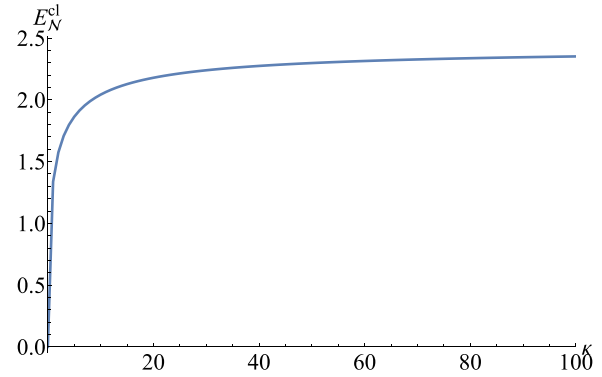


FIG. 9. Classical analog of the logarithmic negativity for two adjacent groups of size $n_1 = n_2 = 10$ in a fixed chain of $N = 500$ oscillators.

hand, for the Bastiaans-Tsallis and Rényi entropies we find that their growth is more negligible for $\alpha > 1$ with respect to the von Neumann entropy. But in the case of $\alpha < 1$, these entropies are much more sensitive to parameter growth than von Neumann entropy.

Regarding the chain of generalized oscillators, the results for the generalized entropies and purities are similar to the case of linearly coupled oscillators in the sense that we can reproduce these results only by taking the corresponding frequencies (30). Furthermore, we have two possibilities for the system to become pure: One implying that the system becomes decoupled, and the other that some self-coupling parameters are imaginary. This last possibility would lead to considering non-Hermitian systems [48,49], showing that quantum entanglement has different characteristics for non-Hermitian systems [50,51], and this situation already appears in our classical context.

In the case of logarithmic negativity, we observe from the worked-out examples that the classical analog (60) gives the same results as the quantum case with the advantage that it can be computed rather easily using only classical information. In this sense, our classical analog can reproduce all the quantum information of Gaussian states. We also corroborate this by comparing the predictions of our approach with the results of [61,62] for a finite system, finding an excellent agreement between them. A remarkable result is that, for the example in Sec. VC and considering $k = 0.0001$, which approaches to the conformal limit of the linear chain, we have obtained an estimation of the value of the central charge from the classical setting. However, as we mentioned the meaning of b_1 in the classical setting demands a more careful analysis.

In view of these results, our classical analogs could be helpful as a first estimation of quantum effects, and it would be worth extending our results to nonintegrable systems, for instance, to compute generalized fractal dimensions [65]. Furthermore, it will be interesting to generalize these classical analogs to other kinds of states, like non-Gaussian states, perhaps along the lines of [66], where quantities like purity are expressed in terms of the Wigner function and of which we have an excellent classical analog.

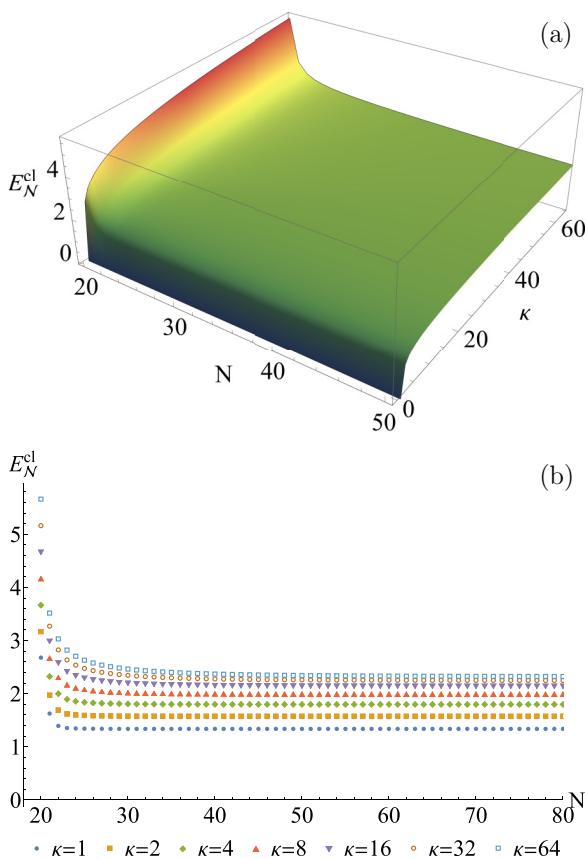


FIG. 8. Classical analog of the logarithmic negativity for two adjacent groups of identical size $n_1 = n_2 = 10$ in a harmonic chain of N oscillators with $k = 0.1$.

ACKNOWLEDGMENTS

This work was partially supported by DGAPA-PAPIIT Grant No. IN105422 and by the Grants No. PID2020-116567GB-C22, No. CEX2019-000904-S funded by No. MCIN/AEI/10.13039/501100011033. B.D. acknowledges support from the CONEX-Plus programme funded by Uni-

versidad Carlos III de Madrid and the European Union's Horizon 2020 research and innovation programme under the Marie Skłodowska-Curie Grant Agreement No. 801538. D.G. acknowledges the financial support under Project SIP-20230323 of IPN. M.J.H. is supported with a CONACyT PhD scholarship (No. 940148).

- [1] S. Amari, *Information Geometry and Its Applications*, Applied Mathematical Sciences (Springer, Japan, 2016).
- [2] G. Jaeger, *Quantum Information: An Overview* (Springer, New York, 2007).
- [3] J. von Neumann and R. Beyer, *Mathematical Foundations of Quantum Mechanics*, Goldstone Printed Materials (Princeton University Press, Princeton, NJ, 1955).
- [4] A. Rényi, *Probability Theory* (North-Holland, Amsterdam, 1970).
- [5] M. J. Bastiaans, New class of uncertainty relations for partially coherent light, *J. Opt. Soc. Am. A* **1**, 711 (1984).
- [6] C. Tsallis, New class of uncertainty relations for partially coherent light, *J. Stat. Phys.* **52**, 479 (1988).
- [7] G. Vidal and R. F. Werner, Computable measure of entanglement, *Phys. Rev. A* **65**, 032314 (2002).
- [8] M. B. Plenio, Logarithmic Negativity: A Full Entanglement Monotone That is not Convex, *Phys. Rev. Lett.* **95**, 090503 (2005).
- [9] M. V. Berry, Quantal phase factors accompanying adiabatic changes, *Proc. R. Soc. London, A: Math. Phys. Sci.* **392**, 45 (1984).
- [10] J. P. Provost and G. Vallee, Riemannian structure on manifolds of quantum states, *Commun. Math. Phys.* **76**, 289 (1980).
- [11] Martin Müller-Lennert, F. Dupuis, O. Szehr, S. Fehr, and M. Tomamichel, On quantum Rényi entropies: A new generalization and some properties, *J. Math. Phys.* **54**, 122203 (2013).
- [12] E. Lenzi, R. Mendes, and L. da Silva, Statistical mechanics based on renyi entropy, *Phys. A (Amsterdam)* **280**, 337 (2000).
- [13] I. Kim, Rényi α entropies of quantum states in closed form: Gaussian states and a class of non-Gaussian states, *Phys. Rev. E* **97**, 062141 (2018).
- [14] P. Jizba and T. Arimitsu, Observability of Rényi's entropy, *Phys. Rev. E* **69**, 026128 (2004).
- [15] C. Tsallis, *Introduction to Nonextensive Statistical Mechanics: Approaching a Complex World* (Springer, New York, 2009).
- [16] E. Lutz, Anomalous diffusion and tsallis statistics in an optical lattice, *Phys. Rev. A* **67**, 051402(R) (2003).
- [17] P. Douglas, S. Bergamini, and F. Renzoni, Tunable Tsallis Distributions in Dissipative Optical Lattices, *Phys. Rev. Lett.* **96**, 110601 (2006).
- [18] G. Wilk and Z. Włodarczyk, Power laws in elementary and heavy-ion collisions, *Eur. Phys. J. A* **40**, 299 (2009).
- [19] V. Khachatryan (CMS Collaboration), Transverse-Momentum and Pseudorapidity Distributions of Charged Hadrons in pp Collisions at $\sqrt{s} = 7$ TeV, *Phys. Rev. Lett.* **105**, 022002 (2010).
- [20] A. Carmi and E. Cohen, On the significance of the quantum mechanical covariance matrix, *Entropy* **20**, 500 (2018).
- [21] R. Horodecki, P. Horodecki, M. Horodecki, and K. Horodecki, Quantum entanglement, *Rev. Mod. Phys.* **81**, 865 (2009).
- [22] K. Audenaert, M. B. Plenio, and J. Eisert, Entanglement Cost under Positive-Partial-Transpose-Preserving Operations, *Phys. Rev. Lett.* **90**, 027901 (2003).
- [23] K. Audenaert, J. Eisert, M. B. Plenio, and R. F. Werner, Entanglement properties of the harmonic chain, *Phys. Rev. A* **66**, 042327 (2002).
- [24] J. H. Hannay, Angle variable holonomy in adiabatic excursion of an integrable Hamiltonian, *J. Phys. A: Math. Gen.* **18**, 221 (1985).
- [25] S. Chaturvedi, M. S. Sriram, and V. Srinivasan, Berry's phase for coherent states, *J. Phys. A: Math. Gen.* **20**, L1071 (1987).
- [26] Z. Yong-de and M. Lei, Berry's phase for coherent states, *II Nuovo Cimento B (1971-1996)* **105**, 1343 (1990).
- [27] J. Gong and P. Brumer, Intrinsic decoherence dynamics in smooth hamiltonian systems: Quantum-classical correspondence, *Phys. Rev. A* **68**, 022101 (2003).
- [28] D. Gonzalez, D. Gutiérrez-Ruiz, and J. D. Vergara, Classical analog of the quantum metric tensor, *Phys. Rev. E* **99**, 032144 (2019).
- [29] J. Alvarez-Jimenez, D. Gonzalez, D. Gutiérrez-Ruiz, and J. D. Vergara, Geometry of the parameter space of a quantum system: Classical point of view, *Ann. Phys.* **532**, 1900215 (2020).
- [30] D. Gonzalez, D. Gutiérrez-Ruiz, and J. D. Vergara, Phase space formulation of the Abelian and non-Abelian quantum geometric tensor, *J. Phys. A: Math. Theor.* **53**, 505305 (2020).
- [31] B. Díaz, D. Gonzalez, D. Gutiérrez-Ruiz, and J. D. Vergara, Classical analogs of the covariance matrix, purity, linear entropy, and von neumann entropy, *Phys. Rev. A* **105**, 062412 (2022).
- [32] J. Evslin and H. Guo, Excited kinks as quantum states, *Eur. Phys. J. C* **81**, 936 (2021).
- [33] V. I. Belinicher, C. Providencia, and J. da Providencia, Instanton picture of the spin tunnelling in the Lipkin - Meshkov - Glick model, *J. Phys. A: Math. Gen.* **30**, 5633 (1997).
- [34] B. Gertjerenken and M. Holthaus, Trojan quasiparticles, *New J. Phys.* **16**, 093009 (2014).
- [35] R. Moreno, V. Carvalho-Santos, D. Altbir, and O. Chubykalo-Fesenko, Detailed examination of domain wall types, their widths and critical diameters in cylindrical magnetic nanowires, *J. Magn. Magn. Mater.* **542**, 168495 (2022).
- [36] M. V. Berry, Semi-classical mechanics in phase space: A study of Wigner's function, *Philos. Trans. R. Soc. London, Ser. A* **287**, 237 (1977).
- [37] M. de Gosson, *Symplectic Geometry and Quantum Mechanics*, Operator Theory: Advances and Applications (Birkhäuser, Basel, 2006).
- [38] L. Diosi, *A Short Course in Quantum Information Theory: An Approach From Theoretical Physics*, Lecture Notes in Physics (Springer, Berlin, 2011).

- [39] G. S. Agarwal, Entropy, the Wigner distribution function, and the approach to equilibrium of a system of coupled harmonic oscillators, *Phys. Rev. A* **3**, 828 (1971).
- [40] A. S. Holevo, M. Sohma, and O. Hirota, Capacity of quantum Gaussian channels, *Phys. Rev. A* **59**, 1820 (1999).
- [41] V. V. Dodonov, Purity- and entropy-bounded uncertainty relations for mixed quantum states, *J. Opt. B: Quantum Semiclassical Opt.* **4**, S98 (2002).
- [42] M. G. A. Paris, F. Illuminati, A. Serafini, and S. De Siena, Purity of Gaussian states: Measurement schemes and time evolution in noisy channels, *Phys. Rev. A* **68**, 012314 (2003).
- [43] T. Golubeva and Y. Golubev, Purity and covariance matrix, *J. Russ. Laser Res.* **35**, 47 (2014).
- [44] A. Serafini, *Quantum Continuous Variables: A Primer of Theoretical Methods* (CRC Press, Boca Raton, FL, 2017).
- [45] M. de Gosson, On the purity and entropy of mixed Gaussian states, in *Landscapes of Time-Frequency Analysis*, edited by P. Boggiatto, E. Cordero, M. de Gosson, H. G. Feichtinger, F. Nicola, A. Oliaro, and A. Tabacco (Springer, Cham, 2019), pp. 145–158.
- [46] T. F. Demarie, Pedagogical introduction to the entropy of entanglement for Gaussian states, *Eur. J. Phys.* **39**, 035302 (2018).
- [47] D. Chruscinski and A. Jamiolkowski, *Geometric Phases in Classical and Quantum Mechanics* (Springer, New York, 2012), Vol. 36.
- [48] C. M. Bender and S. Boettcher, Real Spectra in Non-Hermitian Hamiltonians Having PT Symmetry, *Phys. Rev. Lett.* **80**, 5243 (1998).
- [49] N. Moiseyev, *Non-Hermitian Quantum Mechanics* (Cambridge University Press, Cambridge, 2011).
- [50] S.-L. Chen, G.-Y. Chen, and Y.-N. Chen, Increase of entanglement by local \mathcal{PT} -symmetric operations, *Phys. Rev. A* **90**, 054301 (2014).
- [51] S. Gopalakrishnan and M. J. Gullans, Entanglement and Purification Transitions in Non-Hermitian Quantum Mechanics, *Phys. Rev. Lett.* **126**, 170503 (2021).
- [52] G. Adesso, S. Ragy, and A. R. Lee, Continuous variable quantum information: Gaussian states and beyond, *Open Syst. Inf. Dyn.* **21**, 1440001 (2014).
- [53] R. Bhatia, *Matrix Analysis* (Springer, Berlin, 1997).
- [54] A. Wehrl, The many facets of entropy, *Rep. Math. Phys.* **30**, 119 (1991).
- [55] N. Linden, M. Mosonyi, and A. Winter, The structure of Rényi entropic inequalities, *Proc. R. Soc. A* **469**, 20120737 (2013).
- [56] G. Adesso, A. Serafini, and F. Illuminati, Extremal entanglement and mixedness in continuous variable systems, *Phys. Rev. A* **70**, 022318 (2004).
- [57] Y. S. Kim and M. E. Noz, Coupled oscillators, entangled oscillators, and Lorentz-covariant harmonic oscillators, *J. Opt. B: Quantum Semiclass. Opt.* **7**, S458 (2005).
- [58] J. P. Paz and A. J. Roncaglia, Dynamics of the Entanglement between Two Oscillators in the Same Environment, *Phys. Rev. Lett.* **100**, 220401 (2008).
- [59] D. N. Makarov, Coupled harmonic oscillators and their quantum entanglement, *Phys. Rev. E* **97**, 042203 (2018).
- [60] D. Han, Y. S. Kim, and M. E. Noz, Illustrative example of Feynman’s rest of the universe, *Am. J. Phys.* **67**, 61 (1999).
- [61] P. Calabrese, J. Cardy, and E. Tonni, Entanglement Negativity in Quantum Field Theory, *Phys. Rev. Lett.* **109**, 130502 (2012).
- [62] P. Calabrese, J. Cardy, and E. Tonni, Entanglement negativity in extended systems: A field theoretical approach, *J. Stat. Mech.: Theory Exp.* (2013) P02008.
- [63] J. Kofler, V. Vedral, M. S. Kim, and Č. Brukner, Entanglement between collective operators in a linear harmonic chain, *Phys. Rev. A* **73**, 052107 (2006).
- [64] R. A. Jefferson and R. C. Myers, Circuit complexity in quantum field theory, *J. High Energy Phys.* **10** (2017) 107.
- [65] O. Zmeskal, P. Dzik, and M. Vesely, Entropy of fractal systems, *Comput. Math. Appl.* **66**, 135 (2013).
- [66] M. Walschaers, Non-gaussian quantum states and where to find them, *PRX Quantum* **2**, 030204 (2021).